Research on seismic performance of corrugated web rigid structures

Cao Huimin

(Xi'an Traffic Engineering Institute, Xi·an710072, China)

Abstract: Corrugated steel refers to steel that is wavy along the length direction and is widely used in beams, columns, walls, and other parts of building structures. It plays a connecting and supporting role. The wavy or folded shape of the web plate to some extent improves the shear instability ability and out-of-plane stiffness of the web plate. Industrial factories often use corrugated web H-shaped steel components. However, although corrugated web H-shaped steel components have the advantages of high strength, high stiffness, lightweight, and convenient construction, relevant regulations indicate that these components can only be used for lower intensities or higher intensities when certain conditions are met, One important condition is that the ratio of the design value of axial force including seismic action to the product of the cross-sectional area of the component flange and the design value of steel tensile strength should not exceed 0.4. In this regard, this article will further explore the seismic characteristics and applicable intensity of H-shaped steel structures with corrugated web plates under earthquake action through large-scale finite element ABAQUS simulation. The dynamic characteristics and failure situation of corrugated rigid frame structures will be observed through the elastic-plastic time history analysis method, and the plastic deformation characteristics of steel beam members will be observed by applying low-cycle repeated loads through the hysteresis analysis method. The research shows that under reasonable design conditions, Corrugated web H-shaped steel structural components can be appropriately increased in axial compression ratio for use in high-intensity areas.

Keywords: corrugated web; Intensity; Hysteresis characteristics; TAxial compression ratio

Introduction：

Green building comprehensively implements the concept of green, environmental protection, and energy saving in project construction and construction, and maintains the characteristics of sustainable development, while the development of prefabricated steel structures effectively promotes the development of green building.[1]。

Corrugated steel profile is a new type of green building steel developed in recent decades. due to the accessibility of materials, components can be cut and assembled at the construction site, without waste production and reducing transportation costs. it is favored by researchers because of the advantages such as the possibility of selecting cross-sections according to load.[2]。 With the in-depth exploration of researchers, the statics research of corrugated steel profiles in the construction field has been relatively [1i]mature, and the dynamic research has gradually increased: Qiuhong Zhao

Fund project:1. project of Shaanxi Provincial Department of Education；2.Young and middle-aged project of Xi'an Institute of Communications Engineering

et al proposed a performance-based seismic design (PBSD) method for corrugated steel plate shear wall (CoSPSWs). The results show that the CoSPSW structure designed by the PBSD method shows an ideal yield mechanism, and all the interlayer drift is much lower than the target drift of 2.5%. And the drift distribution is more stable under rare earthquakes[3]. Qirui Luo designed six shear walls for experimental research, analyzing their failure process and mode, magnetic hysteresis diagram, trunk curve, energy consumption capacity, and stiffness degradation, to observe the hysteretic performance of corrugated steel plate composite shear wall[4]； Jing-Shen Zhu introduces the experimental seismic behavior of concrete-filled double steel corrugated plate wall (CDSCW) by applying horizontal cyclic load under constant axial compression. The conclusion of the experimental study provides a basis for the establishment of the CDSW seismic design method.[5]； Bai Zhengxian and others carried out a pseudo-static analysis on the examples of corrugated steel plate shear wall and steel plate shear wall with 13 different parameters such as changing the connection mode, axial compression ratio, and waveform shape with the finite element analysis software ABAQUS, and obtained the failure mode and hysteretic behavior of each steel plate shear wall[6]. Thus it can be seen that the research on the dynamic characteristics of corrugated steel plate in the construction field is mainly focused on corrugated plate shear walls and connectors. Combined with practical investigation, corrugated web profiles have many advantages, but their complex production technology and seismic performance are limited to a certain extent[7][8]. As a result, its promotion and use in China is still insufficient compared with that in Europe and the United States, so the research of the corrugated steel industry and civil buildings in the field of earthquake resistance is of great significance[9].

This paper mainly adopts the method of time history analysis of rigid frames and hysteretic analysis of steel beams using a combination of dynamics and statics[10]. The axial compression ratio of H-shaped steel members with corrugated webs is further discussed to provide a theoretical basis for the application of H-shaped steel members in high-intensity seismic areas.

1 Model establishment

The model of this paper is created by ABAQUS finite element software, and the S4R shell element is adopted. The constitutive model of steel is shown in Figure 1-1, and the material parameters are shown in Table 1-1. Figures 1-2 and Table 1-2 are the zigzag parameters of the web used in this paper.

Tab. 1-1Material Parameters

Steel products	Elastic modulus	Density	Poisson 's ratio	Design value of tensile strength
Q345	$2.06\times10^{11}N/m^2$	7850kg/ m^3	0.28	$310N/mm^2$

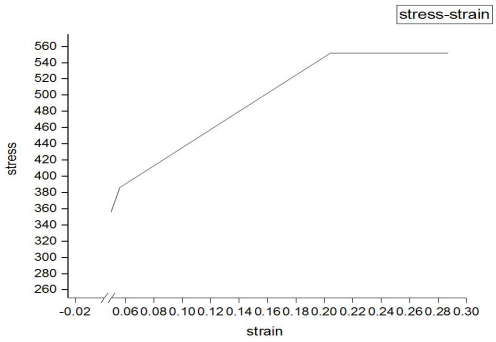

Fig. 1-1 Material Constitutive Model

Fig. 1-2 Web plate bending parameters

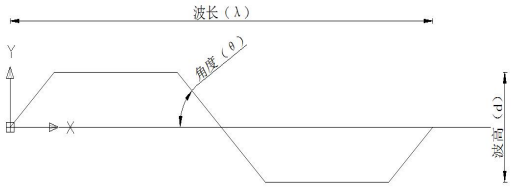

Angle （°）	Wave length （mm）	Wave height (mm)	Flange thickness-to-width ratio	Thickness (mm)	Web height （mm）
45	240	25	0.05	2	520

Tab.1-2 Comparison Table of Geometric Parameters of Component

Model an is a corrugated rigid frame structure with zero slopes of the roof ridge. the lengths of beam members are 6m, 12m, 18m, and 24m respectively, and the column heights are all 6m. The node is just a knot. X, Y, and Z directions are column height direction, perpendicular to beam axis direction and rigid frame span direction respectively; model b is the model of ordinary rigid frame beam members, and the hysteretic characteristics of corrugated steel beam members are observed by loading low cycle reciprocating load.

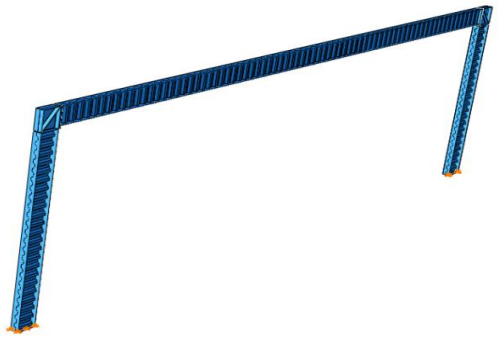

Model a Rigid frame structure model

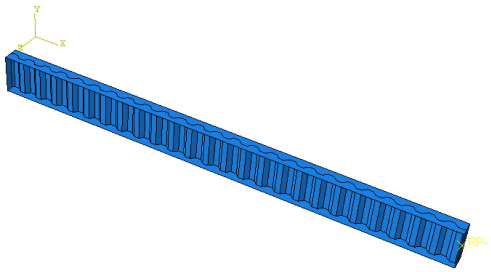

Model b Steel beam structure model

Fig.1-3 Model diagram

2 Modal analysis of rigid frame structure

Taking the rigid frame with a span of 12 meters as an example, the modal analysis of the structure is carried out, and each mode is shown in Fig 2-1.

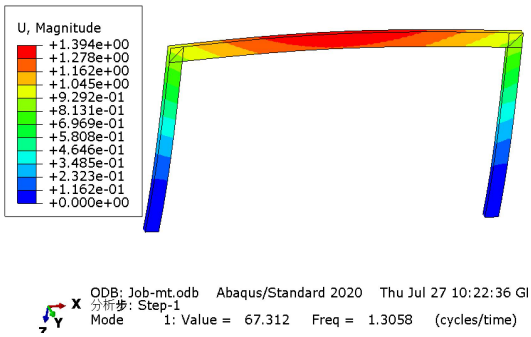

First-order mode

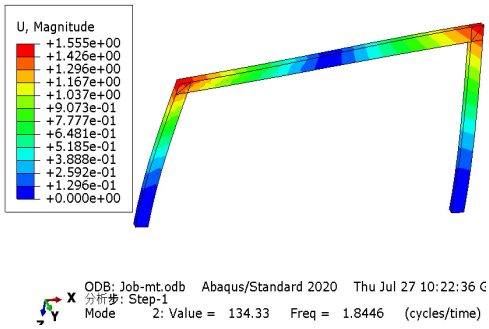

Second-order mode

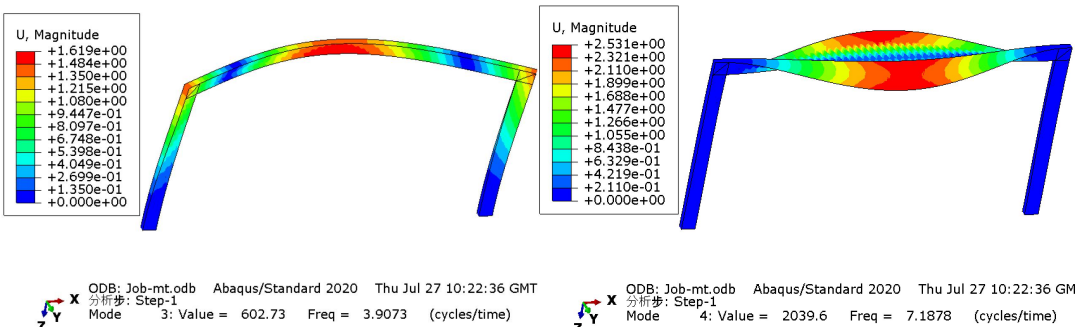

Third-order mode　　Fourth-order mode

Fig. 2-1 Modal Analysis Diagram

In this model, the first four modes are extracted by the subspace iteration method, in which the first frequency is 1.3058HZ, that is, the period of the model is 0.74s. There is little difference between the manual calculation and the software results obtained from the calculation formula $\omega = \sqrt{\frac{K}{M}}$, which shows that the structural model is correct and available.

3 Time history analysis of rigid frame

In the time-history analysis, the beam is simulated as a compression-bending member by applying a pair of eccentric forces, where the axial compression ratio is controlled to be 0.4 and 0.5 respectively, and the formula is used to calculate the axial compression ratio. $n = N / (f * A_f)$, Among them, *N*-the axial pressure value, A_f -the net cross-sectional area of the flange, and f -the design value of steel tensile strength.

The constraint Ux, UR1, UR2, UR3 at the bottom of the column is zero, and Uy and Uz apply EL-Centro seismic wave, through the formula. $a_0(t_i) = \frac{a_{0,\max}}{a_m} a(t_i)$ carry out amplitude modulation， Now take the rare occurrence of EL-Centro wave of degree 7, that is, the peak value of seismic wave as 2.20m/s2, as an example， By amplitude modulation[11]， This is shown in figure 3-1.

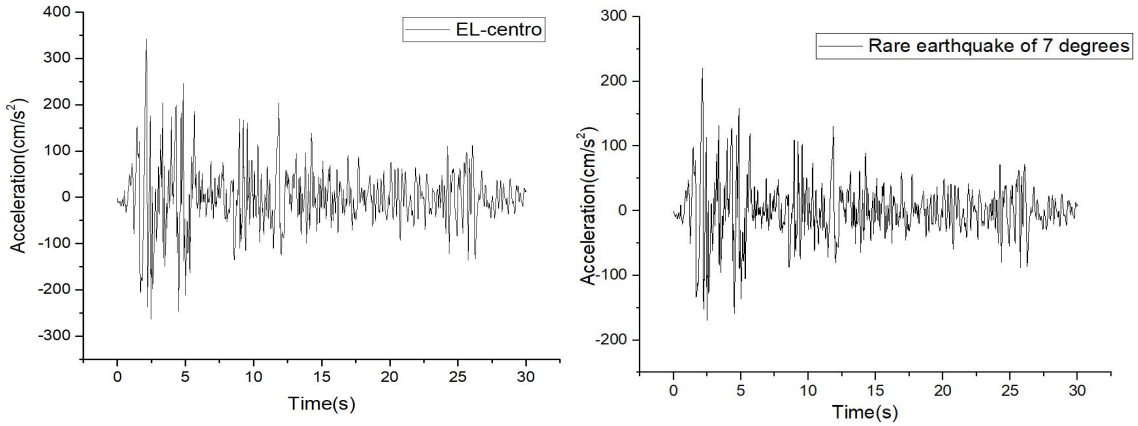

（a） Before the *EL-Centro* Amplitude Modulation　　（b） After the *EL-Centro* Amplitude Modulation

Fig.3-1 Comparison of EL Centro Wave before and after Amplitude Modulation

According to the Stipulate of the the 《Technical Specification for Steel Structures of Lightweight Buildings with Portal Frames》（*GB51022:2015*）[12]： A single-layer portal steel frame, without crane and light steel wallboard, the displacement of the top of the column is not greater than H/ 60, that is, the interlayer displacement angle is not more than 0.017.Tab.3-1 shows that when the beam span is 6m and 12m, it can not meet the area of a 9-degree rare earthquake, while the 18m and 24m span can meet the intensity under different axial compression ratios, and the axial compression ratio has little effect on the inter-story displacement angle. As can be seen in Fig. 3-2 and Fig. 3-3, no matter how much the beam span is, the inter-story displacement and inter-story displacement angle are not affected by the axial compression ratio, and their values are proportional to the intensity of seismic waves.

《Load Code for the Design of Building Structures》 *GB*50009 Regulated: The maximum deflection of bending members should be calculated according to the standard combination of load effect and considering the long-term effect, for roof, floor and staircase components: when $L_0<7m$, the deflection should not exceed $L_0/200(L_0/250)$； when $7\leq L_0\leq 9m$, the deflection should not exceed $L_0/250(L_0/300)$； when $L_0>9m$, the deflection should not exceed $L_0/300(L_0/400)$[13]. Among them, L_0 is the calculated length of the component, and the value in parentheses corresponds to the component that requires higher deflection in use. According to the calculation, the deflection in Tab.3-1 meets the design requirements.

Tab.3-1 Variables Corresponding to Different Seismic Wave

Beam span	Axial compression ratio	Wave peak value	220	310	400	510	620
6m	0.4	(Interlayer displacement) $_{max}$	39.29	54.91	70	89.60	**108.61**
		(Interlayer displacement angle) $_{max}$	0.0065	0.0092	0.0117	0.0149	**0.0181**
		(Mid-span deflection)$_{max}$	5.30	5.46	5.60	5.76	5.90
	0.5	(Interlayer displacement) $_{max}$	39.63	55.20	70.45	89.34	**108.67**

Beam span	Axial compression ratio	Wave peak value	220	310	400	510	620
12m	0.4	(Interlayer displacement angle) $_{max}$	0.0066	0.0092	0.0117	0.0149	**0.0181**
		(Mid-span deflection)$_{max}$	6.65	6.68	6.81	7.10	7.14
		(Interlayer displacement) $_{max}$	40.79	56.36	72.03	91.21	**109.89**
	0.5	(Interlayer displacement angle) $_{max}$	0.0068	0.0094	0.0120	0.0152	**0.0183**
		(Mid-span deflection)$_{max}$	13.51	13.62	13.79	13.92	14.01
		(Interlayer displacement) $_{max}$	41.30	56.51	72.66	91.86	**111.04**
		(Interlayer displacement angle) $_{max}$	0.0069	0.0094	0.0121	0.0153	**0.0185**
		(Mid-span deflection)$_{max}$	16.57	16.72	16.80	16.91	17.07
18m	0.4	(Interlayer displacement) $_{max}$	31.65	42.57	46.57	58.31	81.41
		(Interlayer displacement angle) $_{max}$	0.0053	0.0071	0.0078	0.0097	0.0136
		(Mid-span deflection)$_{max}$	24.98	24.99	25.12	25.68	25.82
	0.5	(Interlayer displacement) $_{max}$	32.70	43.20	54.79	68.57	82.26
		(Interlayer displacement angle) $_{max}$	0.0055	0.0072	0.0091	0.0114	0.0137
		(Mid-span deflection)$_{max}$	30.24	30.33	30.61	30.94	31.10
24m	0.4	(Interlayer displacement) $_{max}$	31.20	41.82	52.35	65.33	78.57
		(Interlayer displacement angle) $_{max}$	0.0052	0.0070	0.0087	0.0109	0.0131
		(Mid-span deflection)$_{max}$	42.47	40.76	41.02	41.27	41.61
	0.5	(Interlayer displacement) $_{max}$	32.48	43.45	53.5	66.40	79.36
		(Interlayer displacement angle) $_{max}$	0.0054	0.0072	0.0089	0.0111	0.0132
		(Mid-span deflection)$_{max}$	50.31	48.03	50.61	50.98	50.14

Note: the peak unit of seismic wave is cm/s^2, and the unit of displacement and deflection is mm.

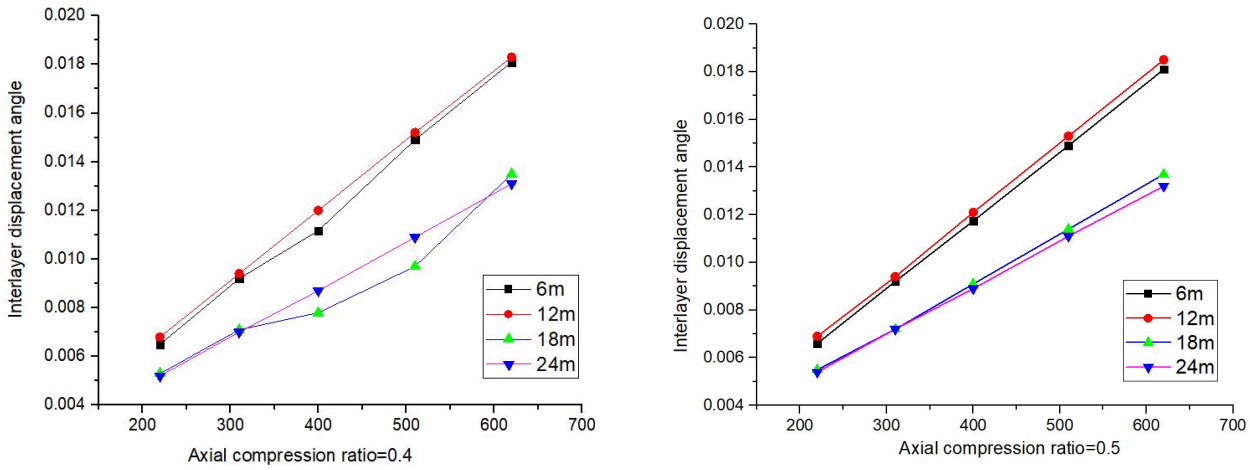

Fig.3-2 Maximum Interstory Displacement Angle

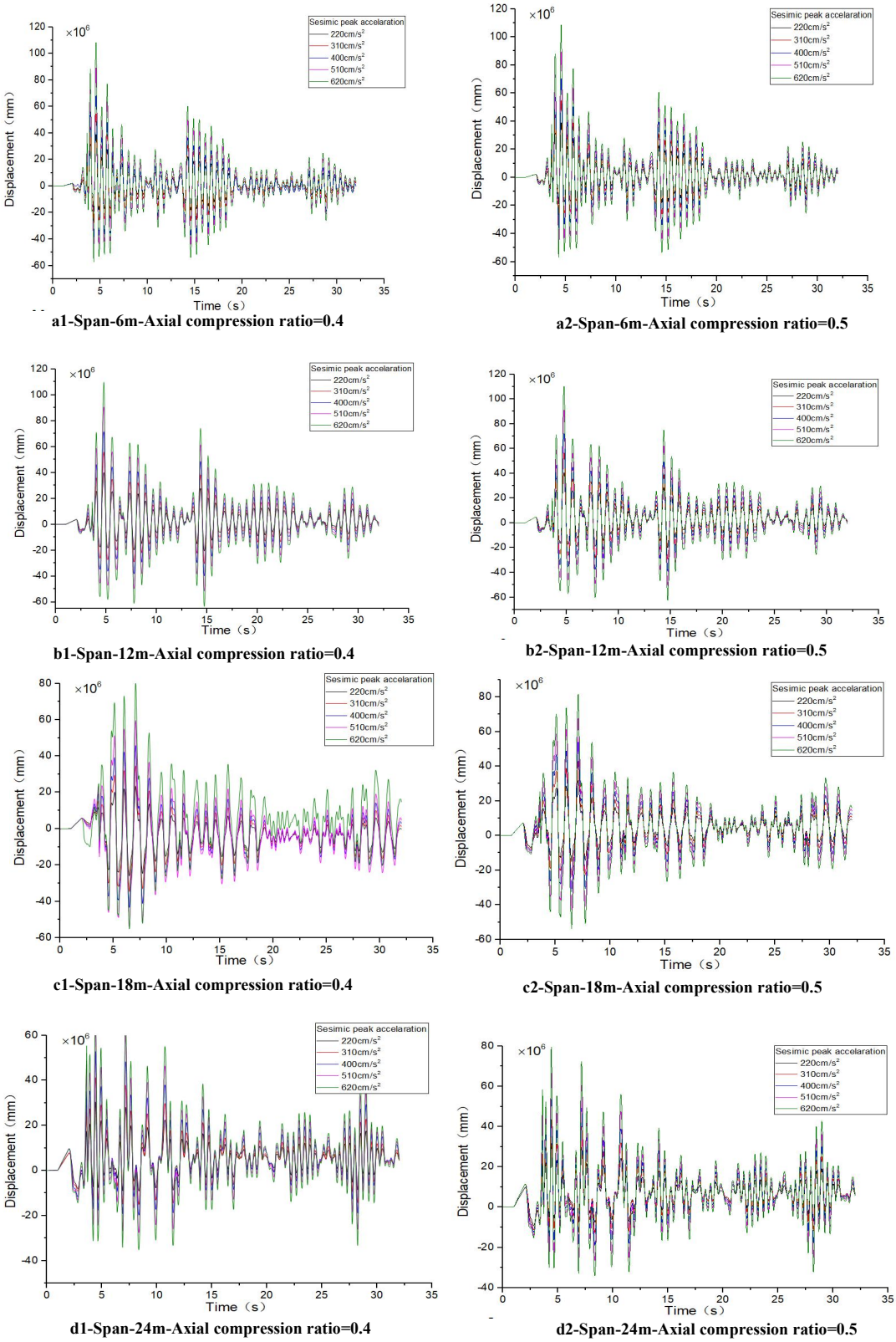

a1-Span-6m-Axial compression ratio=0.4

a2-Span-6m-Axial compression ratio=0.5

b1-Span-12m-Axial compression ratio=0.4

b2-Span-12m-Axial compression ratio=0.5

c1-Span-18m-Axial compression ratio=0.4

c2-Span-18m-Axial compression ratio=0.5

d1-Span-24m-Axial compression ratio=0.4

d2-Span-24m-Axial compression ratio=0.5

Fig.3-3 Time history curves of different spans and axial compression ratios

The greater the earthquake acceleration, the greater the damage to the structure. Here, we tend to observe the force cloud diagram of the member when the intensity is 9 degrees. The cloud

diagram in Tab.3-2 shows that the member does not reach the yield strength when the axial compression ratio is 0.4 and 0.5, And the stress value decreases with the increase of span.

The maximum internal force of the structure is 647.7kN, and the corresponding axial compression ratio is about 0.52. the maximum stress is that 224.9MPa does not reach the yield stress of the structural material, so the structure is not damaged.

Tab.3-2 Cloud Chart of Different Spans and Axial Compression Ratios

Span	The axial compression ratio is 0.4	The axial compression ratio is 0.5
6m	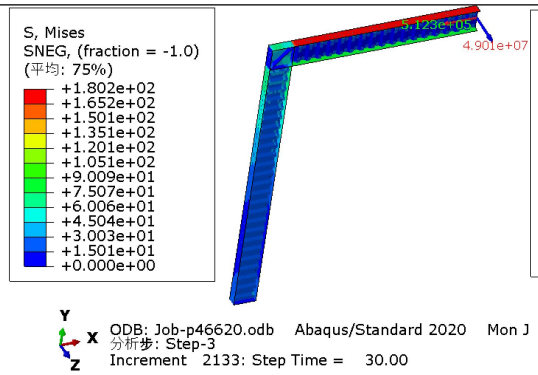	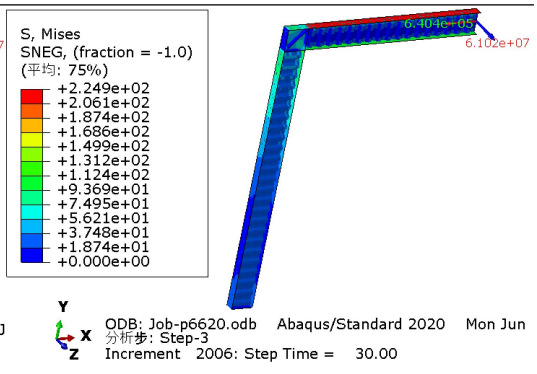
12m	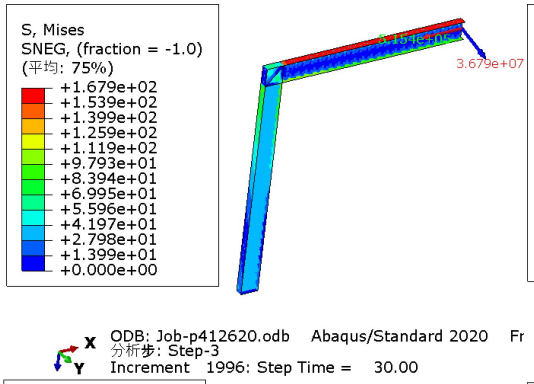	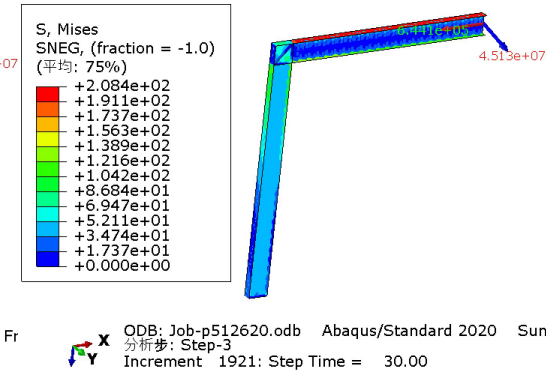
18m	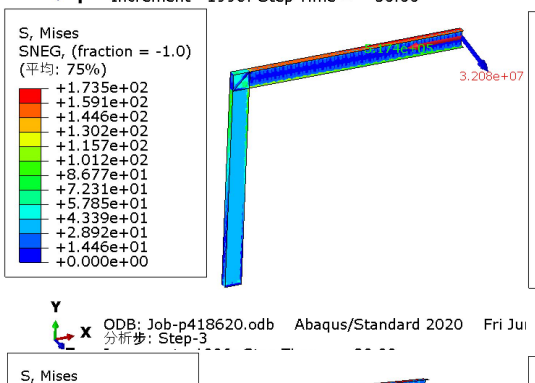	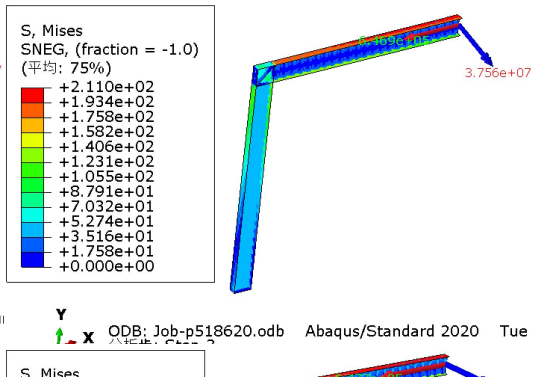
24m	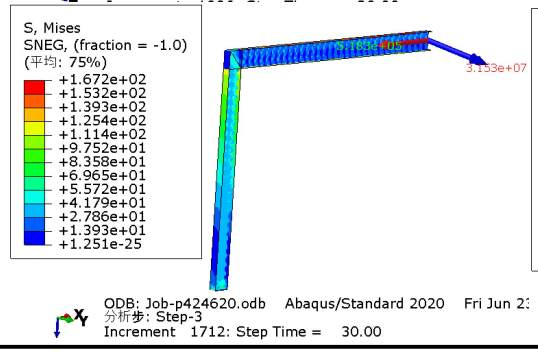	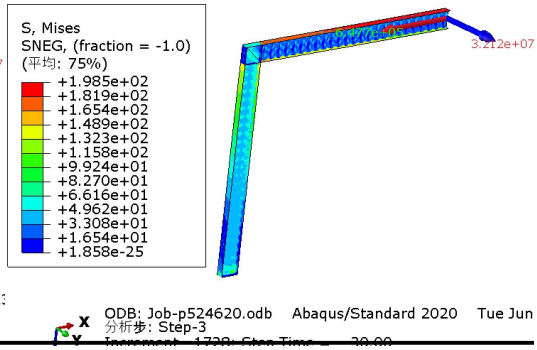

3 Hysteretic analysis

The hysteretic analysis part adopts the simplified mode of complete consolidation at one end, that is, all six degrees of freedom are 0 and loading at the other end. The loading end sets the displacement amplitude of the vertical beam direction applied to the coupling point at the beam end in the boundary condition, starting from 0mm, and loading to 180 mm step by step. At the same time, the corresponding time length of the amplitude is set in the analysis step.[14][15],The loading system is shown in Fig. 3-4.

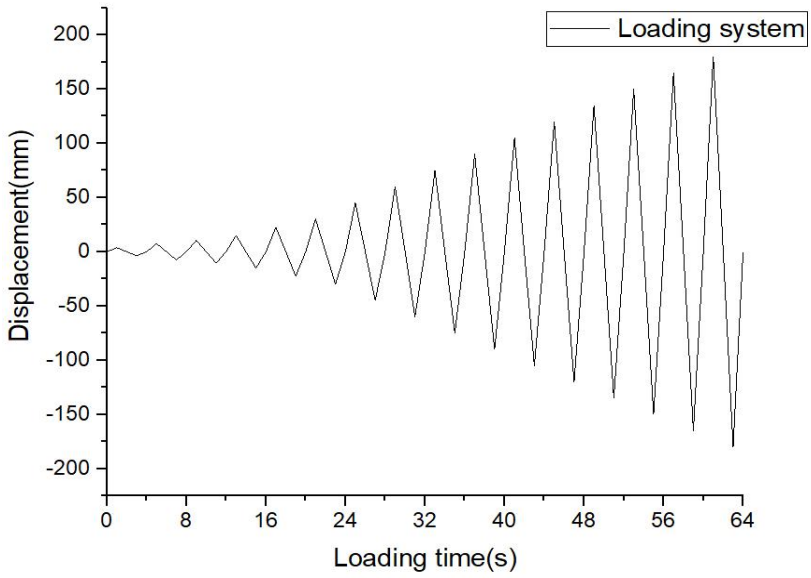

Fig. 3-4 Loading System

From the hysteretic curve and Mises cloud diagram of Tab.3-3, it can be seen that the change in axial compression ratio has little influence on the hysteretic loop. The hysteretic curve is the fullest, slightly pinched, and has the strongest energy dissipation capacity when the beam spans 6m. The skeleton curve goes through three stages of elasticity, elastoplasticity, and plasticity, and the two ends of the beam reach the yield limit and fail[16].

When the beam span is 12m, the hysteretic curve has been pinched, and the beam appears a certain degree of torsion under displacement loading. at this time, the failure point of the steel beam is no longer concentrated at the beam end, but is destroyed by local buckling at the torsion point; with the increase of shear-span ratio, the area surrounded by the hysteretic loop gradually decreases, the pinch-slip of the hysteretic curve is serious, the external force required by the same displacement becomes smaller, and the energy consumption becomes smaller [17].

As can be seen from Tab.3-3, the torsional slip of the member is serious at 18m, while the member with a 24m span is almost in elastic deformation, but the energy dissipation decreases obviously, so the excessive shear-span ratio is not conducive to earthquake resistance.

Tab.3-3 Time Delay Loop Curve and Cloud Chart for Different Axial Pressure Ratios

	Hysteretic curve	Mises cloud picture
6m	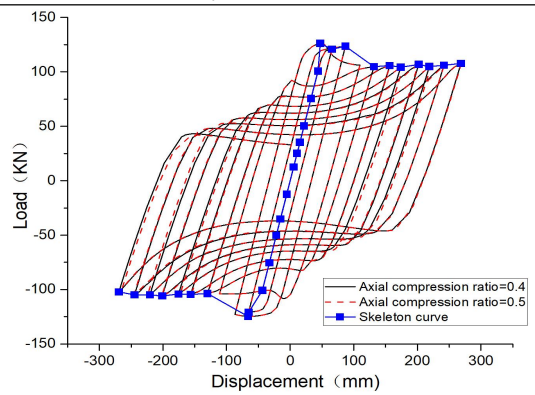	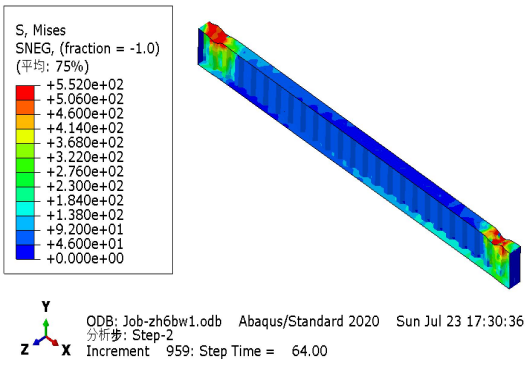
12m	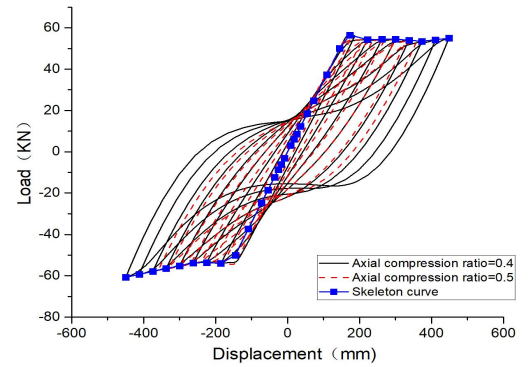	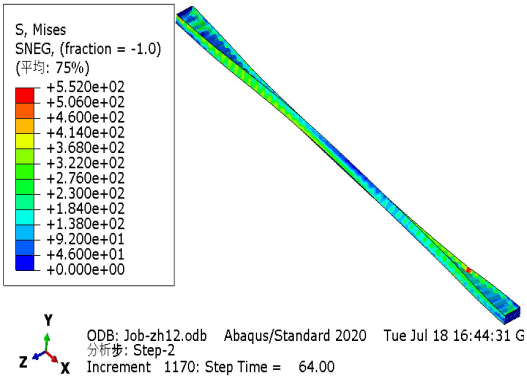
18	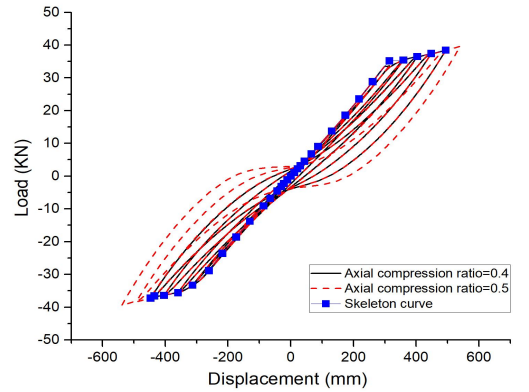	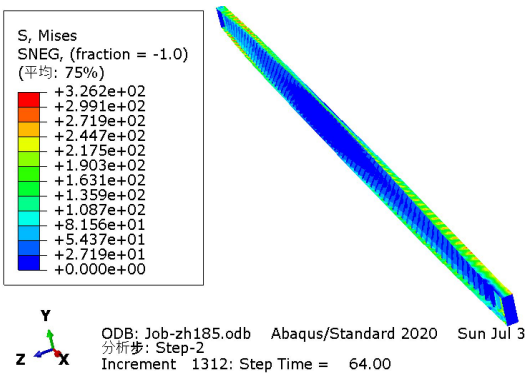
24m	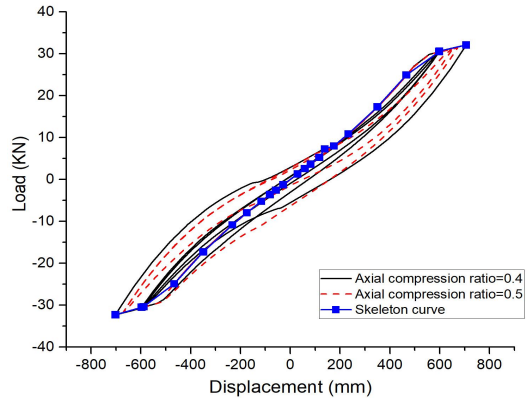	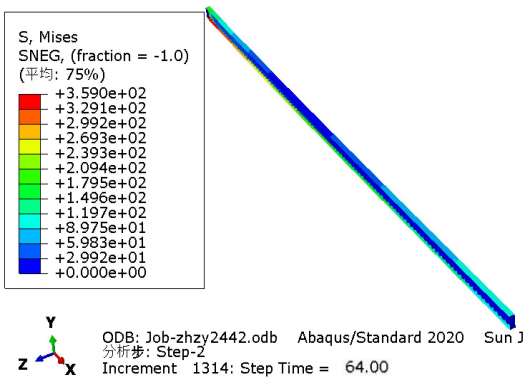

Combined with the above conclusions, we can know:

1. The axial compression ratio has little effect on interlayer displacement and interlayer displacement angle, and the interlayer displacement and interlayer displacement angle increase with the increase of seismic wave intensity.

2.6-24m beam spans can meet rare earthquakes of 8 degrees or less, while 18m and 24m spans can meet rare earthquakes of 9 degrees or less at the same time.

3. When the design is reasonable, the corrugated web steel members can still be used in the seismic intensity area above 7 degrees when the axial compression ratio is 0.52.

4. The axial compression ratio has little influence on the hysteretic performance of the members. With the increase of the span, the members will slip, the hysteretic curve will be pinched, and the energy dissipation will become smaller, which is not conducive to the earthquake resistance of the structure.

Reference:

[1]Chen Haoyu. Analysis and Discussion on the Application of Prefabricated Design and Construction in Green Buildings [J]. China Residential Facilities, 2023 (06): 37-39

[2]IBRAGIMOV A, ZINOVEVA E, ROSINSKIY S. Prefabricated steel structures with a corrugated web (Part 1. Beam)[J/OL]. IOP Conference Series: Materials Science and Engineering, 2020, 869(7): 072041.

[3]ZHAO Q, QIU J, ZHAO Y, et al. Performance-Based Seismic Design of Corrugated Steel Plate Shear Walls[J/OL]. KSCE Journal of Civil Engineering, 2022, 26(8): 3486-3503.

[4]LUO Q, WANG W, SUN Z, et al. Seismic performance analysis of corrugated-steel-plate composite shear wall based on corner failure[J/OL]. Journal of Constructional Steel Research, 2021, 180: 106606.

[5] ZHU J S, GUO Y L, WANG M Z, et al. Seismic performance of concrete-infilled double steel corrugated-plate walls: Experimental research[J/OL]. Engineering Structures, 2020, 215: 110601.

[6]Bai Zhengxian, Cui Hu, Jiang Ziqin, et al. The influence of different parameters on the hysteresis performance of corrugated steel plate shear walls [J]. Industrial Architecture, 2022, 52 (11): 24-31+103. DOI: 10.13204/j.gyjzG21122105

[7]Technical Specification for Application of Corrugated Web Steel Structures (CECS 291:2011) [S] China Planning Press. 2011

[8]Technical Specification for Steel Structures of Lightweight Buildings with Portal Frames (CECS102:2010) [S]. Beijing: China Planning Press

[9]Cheng Jin Analysis on overall stability performance of H-shaped steel axial compression members with corrugated webs [D]. Southwest Petroleum University, 2017

[10]Md S, Carla D, Thomas T. Experimental investigation of the hysteretic behavior of single-story single- and coupled-panel CLT shear walls with nailed connections[J]. Engineering Structures,2023,291.

[11]Hu Yuxian, Earthquake Engineering [M], Beijing, Earthquake Press, 1988: 133 ～ 16

[12]Technical Specification for Steel Structures of Lightweight Buildings with Portal Frames (GB51022:2015) [S]. Beijing: China Planning Press, 2015

[13]Load code for building structures (GB50009-2012) [S]. Beijing: China Construction Industry Press

[14]Wang Mingqing, Zhang Zhi, Chen Zhenhai, et al. Seismic performance analysis of a new type of connection node between embedded wall panels and steel frames [J]. Science and Technology and Engineering, 2023,23 (18): 7868-7877

[15]XUE G, BAO W, JIANG J, et al. Hysteretic Behavior of Beam-to-Column Joints with Cast Steel Connectors[J/OL]. Shock and Vibration, 2019, 2019: 1-20.

[16]Zhang Li, Xu Yafeng Analysis of the Influence of Different Axial Compression Ratios on the Hysteretic Performance of Carbon Fiber Reinforced Steel Reinforced Concrete Filled Steel Tubular Columns [C]//Shenyang Municipal Party Committee, Shenyang Municipal People's Government. 2011:6

[17]Lv Liang, Sun guo-hua, Yang Weixing. Analysis of the influence of axial compression ratio on the hysteretic performance of high-strength concrete composite shear walls with I-shaped steel tube bundles [J]. Journal of Suzhou University of Science and Technology (Engineering Technology Edition), 2023,36 (01): 8-14